

Analysis of Ride Comfort Using SIMULINK for A Passive Suspension System on a Quarter Car Test Rig

A. C. Mitra, S. T. Sayed, S. B. Singh, S. M. Yelgir, R. D. Pawar,
V. N. Chougule

(Mechanical Engineering Department, M.E.S. College of Engineering, Pune University, Pune, India)

Abstract: While the present scenarios in the automotive sector reflect to an extremely challenging atmosphere : fighting hard amongst each other in this fierce battle to outperform and outclass one another, there has been a dire need for something special when it comes to suspension systems. Ride comfort (RC) seems to be an un-confronted zone, though many theories supporting the same have been introduced lately. No road projects a profile that to its entirety seems homogenous and smooth. This has an invariably large effect on the degree of comfort that any driver would sense while driving his/her vehicle. On similar lines; this paper intends to establish a precise correlation between the implemented experiments and corresponding simulation analyses. It takes into consideration various aspects of road profiles as well as the impacting excitations on the incorporated springs, thus eventually to produce a smooth drive effect. The simulation analysis is carried out using MATLAB SIMULINK modelling, incorporating accurate multiple bump inputs using a cam that replicates a natural road profile. The experimental set-up: a Quarter Car Test Rig, uses a Data Acquisition Module (DAQ) to assimilate precise recording and interpretation of experimental readings. The obtained results are validated projecting a correlation factor of 0.96; indicating a positive linear relationship.

Keyword: Correlation coefficient, Damping coefficient, MATLAB-SIMULINK, Ride Comfort(RC), Spring stiffness

I. Introduction

While suspension has an important role in any automobile, it pertains to the very aspect of vehicular interface between the body and the assembly. This indirectly initiates a kind of physical deflection under variable road profiles. Human sensations are accounted mainly by the vertical vibrations; ranging between 4 to 8 Hz; as stated as per standards ISO 2631-1:1997 [1]. The research as presented by Goldman [2] compares the subjective impulses of the human body to vibration motion. It evaluated all the corresponding frequencies where subjects initially perceived vibrations, eventually finding it unpleasant and thus refuse to tolerate it. Katu U. S et. al. [3] has stated that for a period of exposure exceeding 30 to 40 minutes (approx.) on a rough terrain / road will have an adverse effect on the driver, ultimately making the driver feel uncomfortable. Purportedly, Sawant et al. [4] has implicitly stated that vehicle drivers are exposed to ride vibrations enumerating an average of 8 hrs to 10 hrs daily. A. M. Darby et. al. [5] has postulated musculoskeletal disorders were of major concern that resulted in work-time (work input) losses equivalent to almost 4.9 million working days in 2003/2004. In recent times, the objective to avoid such physical disorders and disturbances paved the way for numerous approaches have been employed that work to achieve an optimized ride comfort. Janeway [6] recommends that, as far as automobile and railroad practices are considered, they can be well segmented in to different frequency sensation thresholds, namely in to three domains such as very uncomfortable, uncomfortable and strongly noticeable. Ride comfort rating is determined considering the vibrations transferred at the driver-vehicle interface to the human occupant. For such an analysis and improvement in the comfort levels of vehicle occupants, various methodologies have been proposed and extensive work has been carried out in this domain.

Joao P. C et al. [7] postulated a methodology for the optimization of ride comfort and stability of a vehicle using a flexible multi-body model. His work considers the optimization on the basis of evaluating an optimum ride index or factor that we know as the correlation factor, considering various data points of vehicle acceleration.

Such experimental modes of approach have been the basis of this study that proceed towards validating precisely, the obtained experimental results from the test rig with those illustrated by the SIMULINK software. This procedure was implemented with prerequisites such as NI LabVIEW Data Acquisition Module (DAQ) for the experimentation stage while the software - MATLAB SIMULINK was incorporated for achieving the simulation readings and results. The input to the NI DAQ module was using a CAM that generates a half sine wave bump profile that provides the necessary dynamic motion to the test rig.

Nomenclature

| | | | |
|-------|--------------------------|--------------|--|
| RC | Ride Comfort (m/s^2) | z_s | Sprung mass displacement (mm) |
| k_s | Spring stiffness (N/mm) | z_u | Unsprung mass displacement (mm) |
| k_t | Tyre Stiffness (N/mm) | \dot{z}_s | Sprung mass velocity (m/s) |
| c_s | Damping Coefficient | \dot{z}_u | Unsprung mass velocity (m/s) |
| m_s | Sprung mass (kg) | \ddot{z}_s | Sprung mass acceleration (m/s^2) |
| m_u | Unsprung mass (kg) | \ddot{z}_u | Unsprung mass acceleration (m/s^2) |

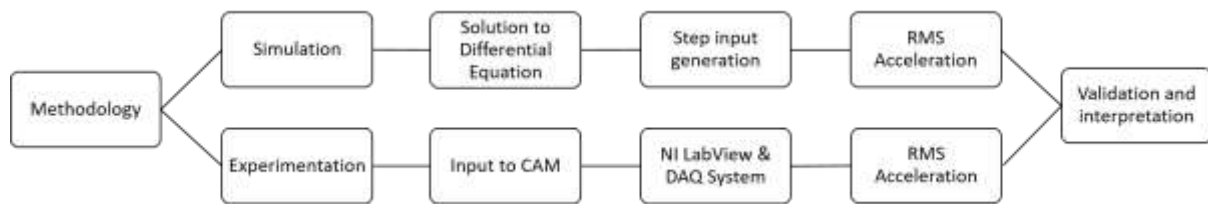


Fig. 1 Schematic flow diagram of various methodologies implemented for RC validation

The variables such as sprung mass (m_s in kg), unsprung mass (m_u in kg), spring stiffness (k_s in N/mm), tyre stiffness (k_t in N/mm) and damping coefficient (c_s) have been incorporated with the help of provisions provided in the test rig itself. Subsequently, Ride Comfort (RC) was measured in terms of Root Mean square (RMS) values of acceleration of the sprung mass and unsprung mass according to the said standards in ISO 2631-1-1997 [1]. Further, the readings and calculations thus obtained from the actual working of the quarter car test rig were fed into the NI LabVIEW system. This is then validated by the simulation done using the MATLAB SIMULINK software. The input parameters such as mass, spring stiffness and damping coefficient can be changed within the program. This process is incorporated with a half sine wave - bump profile as a single road input. With the same methodology, the correlation between the simulation and experimental results is obtained and RC is validated.

1.1METHODOLOGY

This work is directed towards achieving a validated value of RC as far as a passive suspension system is concerned. It focuses on the validation of the SIMULINK model developed with such an accuracy that exactly commensurate to the results obtained in a test rig. The illustration in Fig. 1 explains a hierarchy of stages involved and the process of working out that particular approach. The RMS acceleration values for the validation of RC is carried out by the methodology as illustrated in Fig.1 In the first part of RC analysis, a simulation approach has been employed. It involves the mathematical modelling of a physical system, as in this experiment, a Quarter Car Test Rig. The model is prepared with the help of software such as MATLAB SIMULINK. The Mathematical model of the Quarter Car Test Rig is formulated in to algebraic equations and a SIMULINK Model in MATLAB software is prepared for the same. An important aspect of SIMULINK modelling considered is that, it does not take into consideration parameters such as friction and various suspension geometry factors like camber, castor, KPI, toe, etc. The mathematical model of a passive suspension system is shown in Fig. 2. It is to be observed that the spring and dampers are arranged parallel to each other while the stiffness and damping coefficient cannot be changed or varied i.e. it remains constant. Fig. 3(a) and Fig. 3(b) illustrate the free body diagram of the respective sprung and unsprung masses as well as the independent forces acting on them, viz. Force due to sprung mass (F_s) Force due to unsprung mass (F_u), Force exerted by the tyre (F_t). Equations are obtained for the mathematical model shown in Fig. 2 by the equilibrium method. Applying Newton’s Second Law, the governing equations are formulated as:

1.2 SIMULATION ANALYSIS

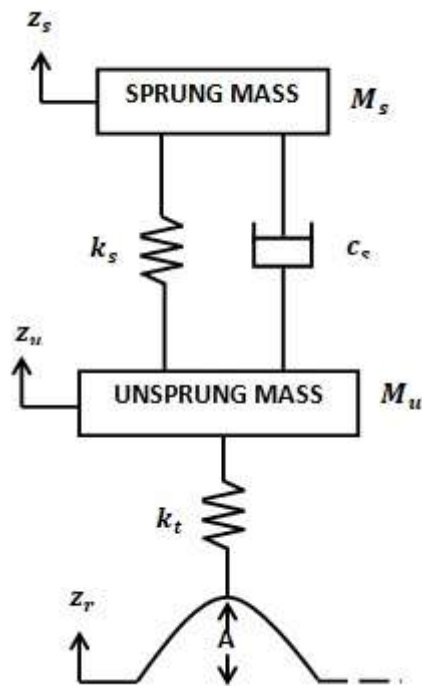


Fig. 2 Model of a Passive Suspension System.

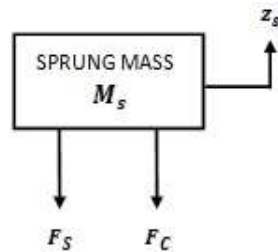


Fig. 3(a) FBD of Sprung mass and its exciting forces.

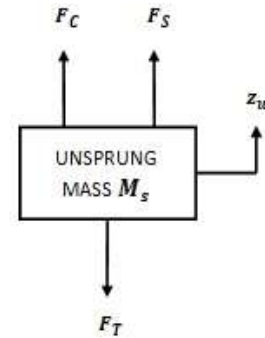


Fig. 3(b) FBD of Unsprung mass and its exciting forces.

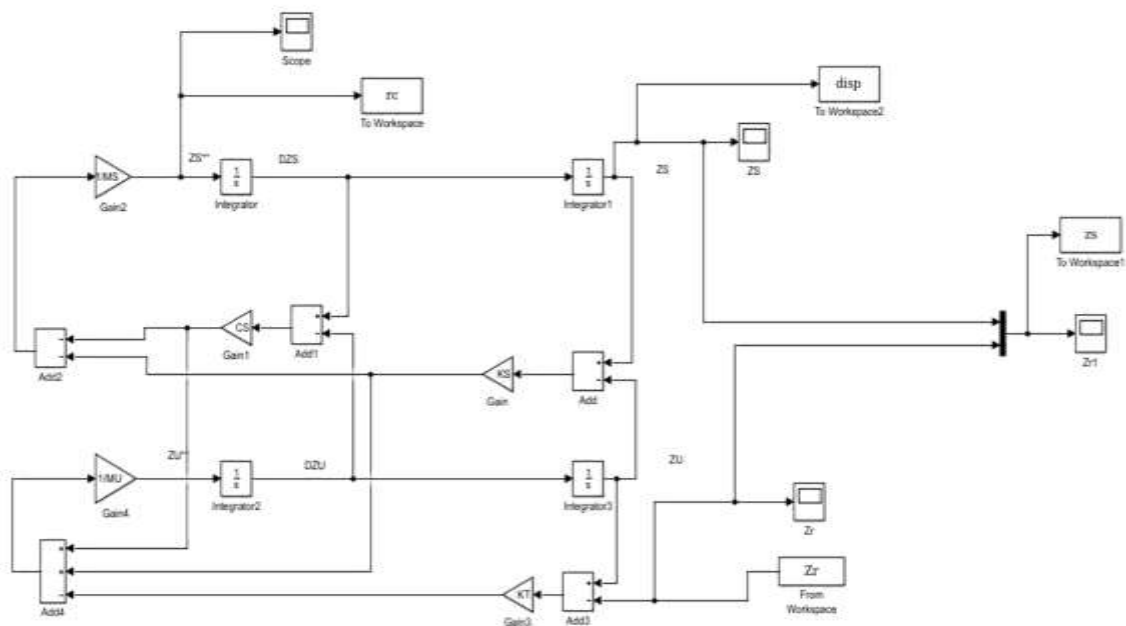


Fig.4 SIMULINK Model generated with actual road input

$$\ddot{z}_s \times m_s = -k_s (z_s - z_u) - c_s \left(\dot{z}_s - \dot{z}_u \right) \tag{1}$$

$$\ddot{z}_u \times m_u = k_s (z_s - z_u) + c_s \left(\dot{z}_s - \dot{z}_u \right) - k_t (z_u - z_r) \tag{2}$$

From the above equations (1) and (2), a MATLAB-SIMULINK program is generated for the linear suspension system as shown in Fig. 4 satisfying equations (1) and (2).

Analysis Of Ride Comfort Using SIMULINK For A Passive Suspension System On A Quarter Car Test Rig

As shown in Fig. 7(a) and Fig. 7(b), the actual road input in the set-up is basically of a half sine wave nature, which is incorporated through a cam. Hence, for a precise output, input to the SIMULINK must be similar to that of the input as in case of the test rig. Fig. 5(a) shows a cam model generated in CATIA V5 R20 that imitates an actual road profile, obtained by literally tracing the cam profile on the test rig. Also, Fig. 5(b) shows the displacement curve for the corresponding road profile which is also created on the CATIA V5 R20 designing software.

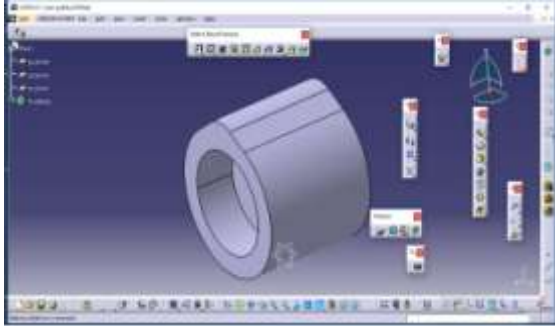


Fig. 5(a) Cam Model imitating an actual road profile.

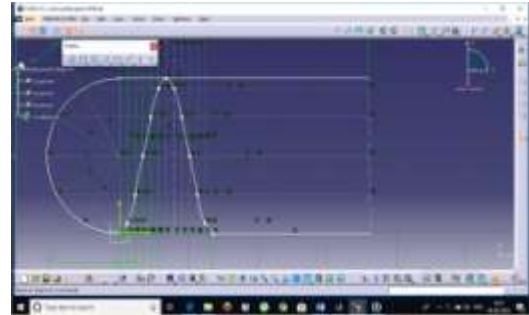


Fig. 5(b) Displacement curve in CATIA V5 R20 road input.

It is hence, observed that the maximum rise of the cam is up to 21 mm for a 65° degree of cam rotation. This cam follows a Rise Return Dwell (RRD) motion to obtain the required half sine wave.

1.1.1. MULTIPLE BUMP INPUT

A further conundrum that arises in this work is that, the generated road input profile is validated as a single - bump road input, however in practise, the nature of the road consists of multiple bumps. Simply we can say giving the same single bump input multiple times. This was achieved using a coded program in MATLAB where two parameters were kept constant; namely time and speed. The multiple bump time-displacement plots are shown explicitly in Fig. 6.

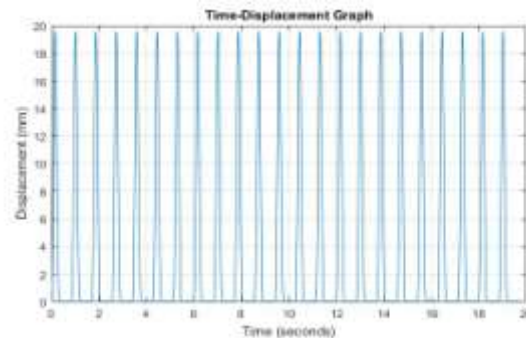


Fig. 6 Plot showing multiple bump road input

II. Experimental Analysis

The experimental analysis involves a developed quarter car test rig. The test rig, as shown in Fig. 7(a) and Fig. 7(b), is then employed with a NI LabVIEW DAQ module. The module is connected to the control computer - PC interface which contains the designed software required to support the experimental interpretations.

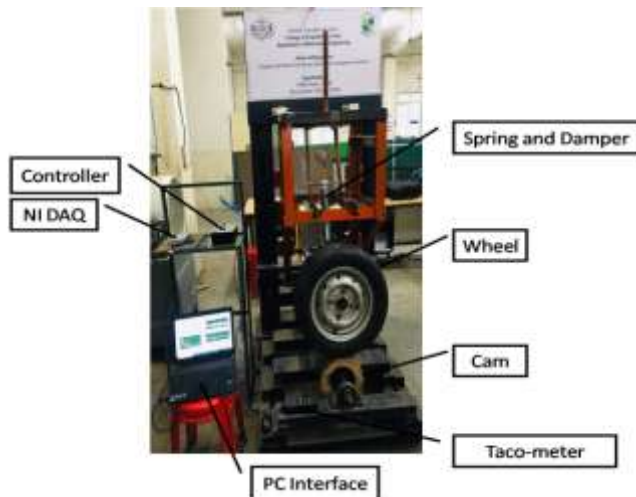


Fig. 7(a) Front view of the quarter test rig integrated with NI hardware and PC interface.

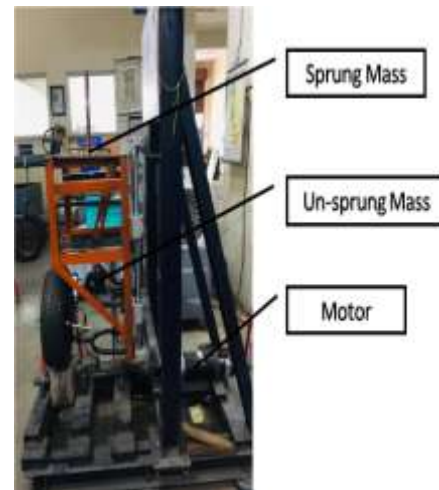


Fig. 7(b) Side view of the quarter test rig with integrated motor.

This test rig uses the displacements that commensurate the actual road nature – bump profile corresponding to the cam motion. The system incorporates the NI LabVIEW DAQ module and various instruments such as a three axes accelerometer, a tachometer and a motor controller for controlling the variation in working conditions such as the operating speed (in RPM) and used springs. The NI LabVIEW DAQ makes it much simpler to acquire and store values required for the validations with the simulations. It generates direct values of sprung acceleration i.e. RMS acceleration.

1.1.2. NI LABVIEW BLOCK PROGRAMMING

The NI LabVIEW block programming is reflected in Fig. 8. This is mainly incorporated to evaluate the values of RMS acceleration for both sprung and unsprung masses, for a time specific duration. As illustrated in Fig. 8, the DAQ Assistant block represents the NI 9234 DAQ Module that is responsible for data assimilation from the test rig. The RMS acceleration for respective sprung and unsprung masses is represented in a much efficient time domain plot. Fig. 9 shows the NI LabVIEW output screen.

1.1.3. DAQ MODULE (DATA ACQUISITION MODULE)

NI 9234 DAQ Module is used as an interface between the computer system containing NI LabVIEW software and the physical vibrating entity upon which the accelerometers are mounted. It is highly sensitive and huge number of readings can be processed in the module. The three-axis accelerometer is connected to the 'A0' port and the single axis accelerometer is connected to the 'A1' port of the accelerometer module used. As the accelerometers are mounted on two mentioned masses and connected to the computer via the DAQ module, direct values of acceleration are obtained on the output screen. As illustrated in Fig. 9, the red line in the frequency domain graph indicates the acceleration of the sprung mass and the white line indicates the acceleration of the unsprung mass while the adjoining graph represents the plot of corresponding sprung and unsprung mass accelerations in a time domain analysis using the Fourier transformation. Various RMS values are obtained, as shown in Table 1, via the experimentations and simulations at different operating speeds (in RPM). Based on this chart, a suitable graph is plotted which represents the RMS values from the experimental and simulation methodologies. With this, the correlation factor is obtained between these two modes, as shown in Fig 10.

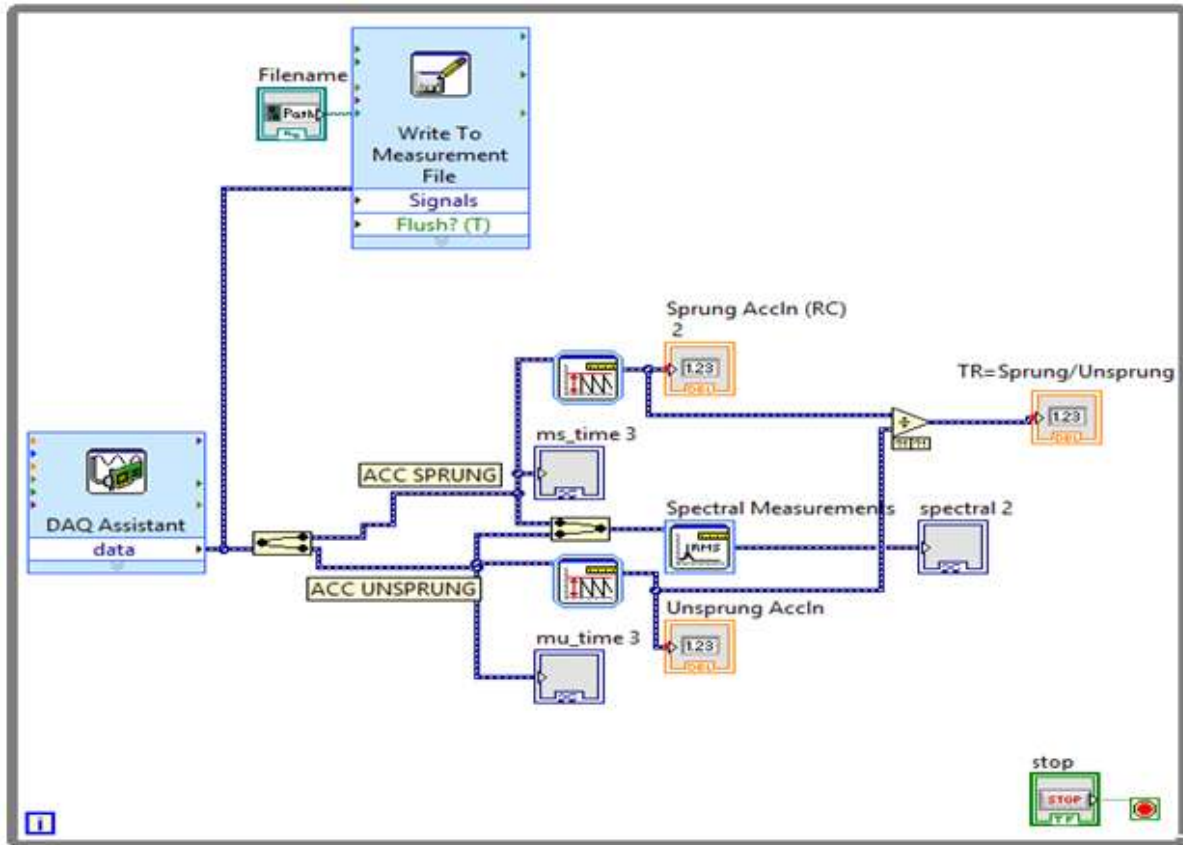


Fig. 8 NI LabVIEW Block diagram for acceleration

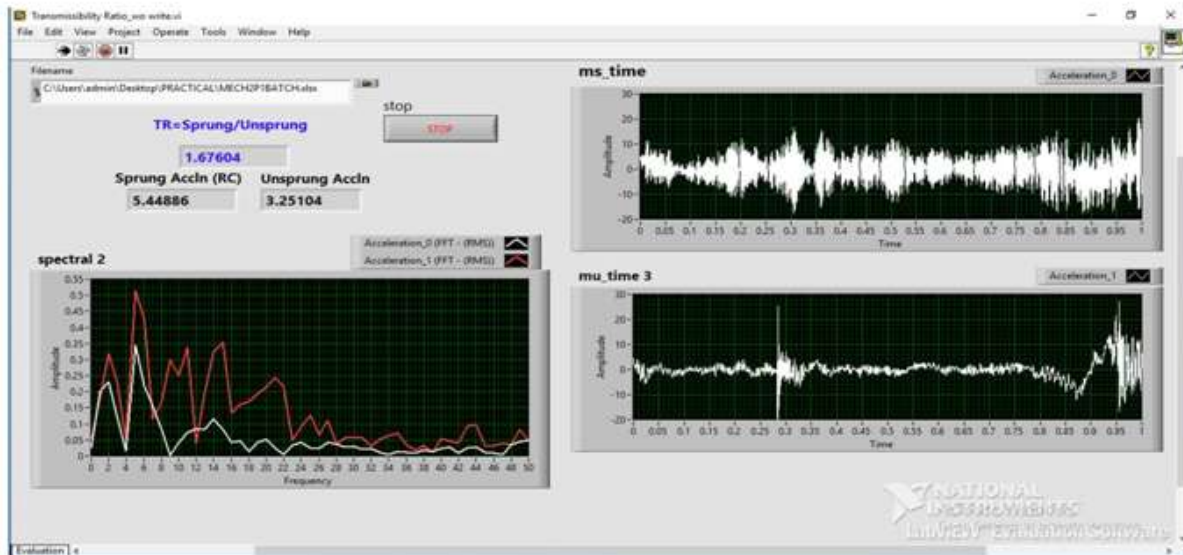


Fig. 9 NI LabVIEW front panel graph validation for acceleration.

III. Results and Discussion

Table 1. Experimental and SIMULINK results of RMS acceleration for various operating speeds.

| Speed (in RPM) | X (Experimental RMS (m/s^2)) | Y (Simulink RMS (m/s^2)) |
|----------------|----------------------------------|------------------------------|
| 30 | 1.6839 | 0.16749 |
| 40 | 2.2259 | 0.3361 |
| 50 | 2.3208 | 0.6101 |
| 60 | 2.6008 | 0.9529 |
| 70 | 2.9716 | 1.3256 |
| 80 | 3.286 | 1.74 |

| | | |
|-----|--------|--------|
| 90 | 3.6446 | 2.1034 |
| 100 | 3.7737 | 2.1411 |
| 110 | 3.9632 | 2.7932 |
| 120 | 4.1127 | 3.1397 |
| 130 | 4.2323 | 3.4352 |
| 140 | 4.6265 | 3.6981 |
| 150 | 5.039 | 3.8712 |
| 160 | 5.4482 | 3.9997 |
| 170 | 6.3477 | 4.1478 |
| 180 | 5.8754 | 4.2515 |
| 190 | 5.6073 | 4.3773 |

The correlation factor, which is denoted by ‘r’, is simply a measure of coherence between any two specific data points under comparison. It is said to assume any value between the formulated intervals of -1 up to +1, including both the extremes. Correlation factor or commonly stated as coefficient, having a value 0 indicates absence of a linear relationship between any two specific points of comparison. The value +1 is an indicator of a perfect positive linear relationship, which explains that as one variable such as X increases in its values, the other variable say Y also increases with an exact linear rule; Table 1 depicts a similar nature of coherence. The value -1 establishes a reverse relationship as that of +1, though satisfying the exact linear rule; as variable X decreases so does variable Y. Correlation coefficient is calculated by expressing the compared values with their means equal to zero and their standard deviations equal to 1 (zX_i and zY_i), as show in equations (1) and (2). These values are rearranged in form of standardized pairs and re-expressed, thus formulating the correlation factor ‘r’:

$$zX_i = [X_i - \text{mean}(X)] / S.D(X) \tag{1}$$

$$zY_i = [Y_i - \text{mean}(Y)] / S.D(Y) \tag{2}$$

$$\therefore r_{X,Y} = \text{Sum of } [zX_i \times zY_i] / (n - 1) \tag{3}$$

The correlation coefficient is thus obtained from the relation as expressed in equation (3), where ‘n’ refers to the considered sample size [11]. Table 2 illustrates the compared values i.e. Experimental RMS acceleration (X_i) and SIMULINK RMS acceleration (Y_i).

Table 2. Corresponding values for X and Y to evaluate the correlation factor.

| Xi (Experimental RMS (m/s ²)) | Yi (Simulink RMS (m/s ²)) | zXi | zYi | zXi * zYi | r(X,Y) |
|---|---------------------------------------|----------|----------|-----------|----------|
| 1.6839 | 0.16749 | -1.67331 | -1.61088 | 2.695503 | |
| 2.2259 | 0.3361 | -1.27933 | -1.49614 | 1.914056 | |
| 2.3208 | 0.6101 | -1.21035 | -1.30969 | 1.585174 | |
| 2.6008 | 0.9529 | -1.00681 | -1.07642 | 1.083747 | |
| 2.9716 | 1.3256 | -0.73727 | -0.8228 | 0.606627 | |
| 3.286 | 1.74 | -0.50873 | -0.5408 | 0.275125 | |
| 3.6446 | 2.1034 | -0.24806 | -0.29351 | 0.07281 | |
| 3.7737 | 2.1411 | -0.15422 | -0.26786 | 0.041309 | |
| 3.9632 | 2.7932 | -0.01647 | 0.175886 | -0.0029 | 0.969421 |
| 4.1127 | 3.1397 | 0.092202 | 0.411675 | 0.037957 | |
| 4.2323 | 3.4352 | 0.17914 | 0.61276 | 0.10977 | |
| 4.6265 | 3.6981 | 0.465688 | 0.79166 | 0.368666 | |
| 5.039 | 3.8712 | 0.765537 | 0.909452 | 0.69622 | |
| 5.4482 | 3.9997 | 1.062988 | 0.996895 | 1.059688 | |
| 6.3477 | 4.1478 | 1.716843 | 1.097675 | 1.884536 | |
| 5.8754 | 4.2515 | 1.373524 | 1.168242 | 1.604608 | |
| 5.6073 | 4.3773 | 1.17864 | 1.253847 | 1.477834 | |
| Mean (X) = 3.985859 | Mean (Y) = 2.534729 | | | | |

Analysis Of Ride Comfort Using SIMULINK For A Passive Suspension System On A Quarter Car Test Rig

Fig. 10 shows the plot of the SIMULINK and the experimental values thus obtained. This relationship gives the degree of exactness or accuracy of the RMS solution obtained, thus validating the modes of analysis and presenting an accurate and optimum value of RC.

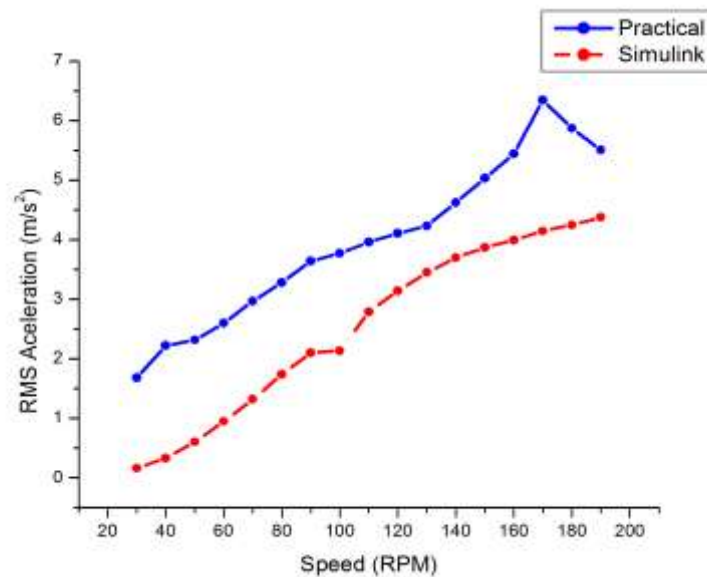


Fig. 10 Plot of RMS acceleration versus speed (in RPM).

IV. Conclusion

The road input developed in MATLAB SIMULINK proved to be an ideal solution as an input to the SIMULINK model which resulted in precise RMS values. The NI LabVIEW block programming also proved to be very efficient in data assimilation, allowing for accurate experimental RMS values that ensured excellent validation results. Correlation coefficient, which is a statistical relation between two comparable data points, was estimated and validated close to a value of 0.96 when RMS was plotted with respect to RPM, which explicitly demonstrates a positive linear relationship. This positive value indicates that there is a positive association; as the value of variable X increases, the value of the corresponding variable Y also increases, in accordance with the exact linear rule.

V. Future Scope

This paper aims to achieve a more optimized value of RC for improving the spring stiffness incorporated in the Passive Suspension System considering various attributes such as camber, castor, and toe changes using the Design of Experiments (DOE) approach. To validate the obtained RC, experimentations such as on-road measurement of governing parameters, and hence optimizing the RC to obtain the most efficient values for springs and dampers on such road profiles. Re-validation after optimization and final testing shall produce assured values, ready for embodiment. Use of dampers will also prove to be a crucial aspect in the analysis and evaluation of an optimum damping coefficient to enhance Road Comfort (RC) and Road Holding (RH) parameters.

Acknowledgements

We are extremely grateful to the MESCOE - NI LabView Academy Lab, Department of Mechanical Engineering, Modern Education Society's College of Engineering, Pune, INDIA for its conscientiousness, exhorting us during the entire course of our research.

Conflict of interest The authors declare that there is no conflict of interests regarding the publication of this paper.

References

- [1]. ISO 2631-5:2018(en), Mechanical Vibration and Shock – Evaluation of Human Exposure to Whole Body Vibration -Part 5: Method for evaluation of vibration containing multiple shocks, 2018-07, Pages 1-33.
- [2]. D.E. Goldman, A Review of the Subjective Response to Vertical Motion of the Human Body in the Frequency Range 1 To 70 Cycles per Second, Naval Medical Research Institute, Report No. 1, March 16, 1948.
- [3]. U.S. Katu, R.G. Desavale and R.A. Kanai, Effect of Vehicle Vibration on Human Body – RIT Experience (Rajaram Bapu Institute of Technology Sakharale Jan 2009).

Analysis Of Ride Comfort Using SIMULINK For A Passive Suspension System On A Quarter Car Test Rig

- [4]. S. H. Sawant, M. V. Belwalkar, M. A. Kamble, P. B. Khot & D. D. Patil, Vibrational Analysis of Quarter Car Vehicle Dynamic System Subjected to Harmonic Excitation by Road Surface, Undergraduate Academic Research Journal (Uarj), ISSN: 2278 – 1129, Volume-1, Issue-1, 2012.
- [5]. A. M. Darby, Whole-Body Vibration and Ergonomics Toolkit - Phase 1 (Published by the Health and Safety Executive, 01/08/2008).
- [6]. R.N. Janeway, Vehicle Vibration Limits to Fit the Passenger, SAE Technical Paper, 1948.
- [7]. J. P. C. Goncalves and J. A. C. AmbroSio, Road Vehicle Modeling Requirements for Optimization of Ride and Handling, Multibody System Dynamics (2005), 13: 3–23 C _ Springer 2005.
- [8]. M. Javad, M. Mohammadi and S. Mostaani, Optimization of a Passive Vehicle Suspension System for Ride Comfort Enhancement with Different Speeds Based on the Design of Experiment Method (DOE) Method, Vol. 5(3), Pp. 50-59, March 2013, Doi 10.5897/Jmer10.061, ISSN 2141-2383 © 2013 Academic Journals.
- [9]. Anirban C. Mitra, Kiranchand G. R., Tanushri Soni, Nilotpal Banerjee, Design of Experiments for Optimization of Automotive Suspension System Using Quarter Car Test Rig, Procedia Engineering, 144 (2016), PP 1102 – 1109.
- [10]. A. C. Mitra, G. R. Kiranchand, S. B. Dhakare, M. S. Jawarkar, Optimization of Passive Suspension System for Enhancement of Ride Comfort, IOSR Journal of Mechanical and Civil Engineering (IOSRJMCE), e-ISSN: 2278-1684, p-ISSN: 2320-334X, PP 01-08.
- [11]. Bruce Ratner, Journal of Targeting, Measurement and Analysis for Marketing (2009), Springer Journal, Volume 17, PP 139 – 142, Doi: 10.1057/jt, 2009; published online 18 May 2009.